Chapter 12

Low-Frequency Noise and Resistance as Reliability Indicators of Mechanically and Electrically Strained Thick-Film Resistors

Zdravko Stanimirović

Additional information is available at the end of the chapter

http://dx.doi.org/10.5772/intechopen.69441

Abstract

New contemporary applications of thick resistive films are inducing the need to investigate their behaviour under various stressing conditions. On the other hand, there is a growing interest in noise measurements as means of thick-film resistor quality and reliability evaluation and evaluation of degradation under stress. For these reasons, this chapter presents effects of mechanical, electrical and simultaneous mechanical and electrical straining on performances of conventional thick-film resistors that are analysed from micro- and macro-structural, charge transport and low-frequency noise aspects.

Keywords: thick-film resistors, mechanical straining, high voltage pulse stressing, resistance, gauge factor, noise index

1. Introduction

Present miniaturization trends and ongoing usage of thick-film resistors in sensitive telecommunications equipment have induced the need to investigate their reliability under various straining conditions. The most of the published data dealt with effects of mechanical straining on performances of these complex heterogeneous systems using the piezoresistive effect in thick resistive films for strain gauge realization [1, 2]. On the other hand, performances of standard thick resistive films subjected to unwanted mechanical straining [3–5] have not been sufficiently investigated despite the fact that mechanical straining may take place during all phases of resistor realization, examination and application. In case of high-voltage pulse stressing, the most of the papers investigated effects of trimming of thick resistive films by energy of high-voltage pulses [6–8] and behavioural analysis of surge thick-film resistors [9].

Influence of electrical straining on the reliability of conventional thick resistive films has been seldom investigated. Little attention has particularly been paid to examining effects of the simultaneous impact of these two types of straining with respect to their contrasting effects on resistor performances. In addition, standard low-frequency noise measurements [10–13] are being recognized as useful tools in reliability analysis of thick-film resistors subjected to various straining conditions. For these reasons, this chapter focuses on performance analysis of mechanically, electrically and simultaneously mechanically and electrically strained thick-film resistors based on compositions with three different volume fractions of conducting phase, using standard resistance and low-frequency noise measurements as valuable indicators in reliability evaluation of thick resistive structures under a wide range of extreme working conditions.

2. Mechanically strained thick-film resistive structures

Thick resistive films have been known for their piezoresistive properties for more than 40 years. Over the years, strain gauge applications have been topics of the most of the available published data. At first, only the basic piezoresistive characteristics of thick resistive films were examined. Later on, new resistive sensing elements emerged based on novel thick-film inks designed for each specific application [14, 15]. On the other hand, standard thick-film resistors are being continuously used in contemporary electronic equipment that requires high functional capability, improved reliability and environmental stability. These up-to-date applications induced the need to examine performances of standard mechanically strained thick-film resistive structures [5, 16].

Sensitivity of a certain material to mechanical strain is referred as the gauge factor. In case of thick-film resistive structures, gauge factor (GF) is defined as the ratio of the relative resistance change ($\Delta R/R$) and the relative change of length of the resistor ($\varepsilon = \Delta l/l$) under influence of mechanical straining:

$$GF = \frac{\Delta R/R}{\varepsilon}. \tag{1}$$

The relation between strain and resistor position on the substrate can be given by the equation [17]:

$$\varepsilon = 12\frac{t\bar{x}}{L^3}d_i,\ d \ll L, \tag{2}$$

where t is substrate thickness, $\bar{x}$ is average position of the thick resistive film with respect to the fixed substrate edge, d is substrate deflection and L is distance between fixed substrate edges. The maximum value for the strain occurs for $\bar{x} = L/2$:

$$\varepsilon_{\max} = \Delta l/l = \frac{6\,d_i\,t}{L^2}. \tag{3}$$

http://dx.doi.org/10.5772/intechopen.69441

Schematic presentation of mechanically strained thick-film resistor is given in **Figure 1**.

Mechanical straining causes a reversible resistance change in thick-film resistors [5, 16]. The reversible resistance change is partially due to change in resistor geometry but mainly due to micro-structure changes. According to 3-D planar random resistor network model [18], transport of electrical charges in thick-film resistive materials takes place via a complex conductive network formed during firing by sintering metal-oxide particles (usually combination of RuO_2 and $Bi_2Ru_2O_7$) immerged in the glass matrix. During the sintering process, a number of conducting chains is being formed. These chains consist of clusters of particles (particles that are in contact) and neighbouring particles separated by thin glass barriers (metal-insulator-metal or MIM units). Therefore, the current flow is being determined by metallic conduction and tunnelling through glass barriers. The micro-structure of thick resistive films, determined by the ratio of the conducting and insulating phase, also determines conducting mechanisms present in the film. Performed experiments [16], illustrated by data given in **Table 1**, showed that gauge factor values are greater for resistors realized with compositions with higher sheet resistances, that is, resistor compositions with smaller volume fractions of conducting phase have greater *GF* values. Thick-film resistors based on compositions with high sheet resistances (≥100 kΩ/sq) have lower volume fraction of conducting phase and therefore charge transport is predominantly limited by tunnelling through glass barriers. Resistors based on compositions with low sheet resistances (≤1 kΩ/sq), because of their high volume fraction of conducting phase, are predominantly limited by conducting through clusters of conducting particles and sintered contacts. Resistors realized using compositions with medium values of sheet resistances, such as 10 kΩ/sq compositions, incorporate approximately equally all above-mentioned charge transport mechanisms. Substrate deflection causes resistance increase due to change of charge transport conditions and greatest resistance change leads to greatest *GF* value. Conducting mechanism known as tunnelling through glass barriers is predominantly influenced by mechanical stressing. The bulk modulus of borosilicate glasses is typically between 40 and 80 GPa [19] while RuO_2 conducting phase has a bulk modulus of approximately 270 GPa. Since the glass phase is less stiff than the conducting one, tunnelling through glass barriers is more sensitive to the applied straining than conduction through conducting particles and sintered contacts between them. Mechanical straining changes dimensions of the thick resistive film. It cannot alter a number of chains, barriers or contacts in the conducting network. Also, it cannot induce dielectric

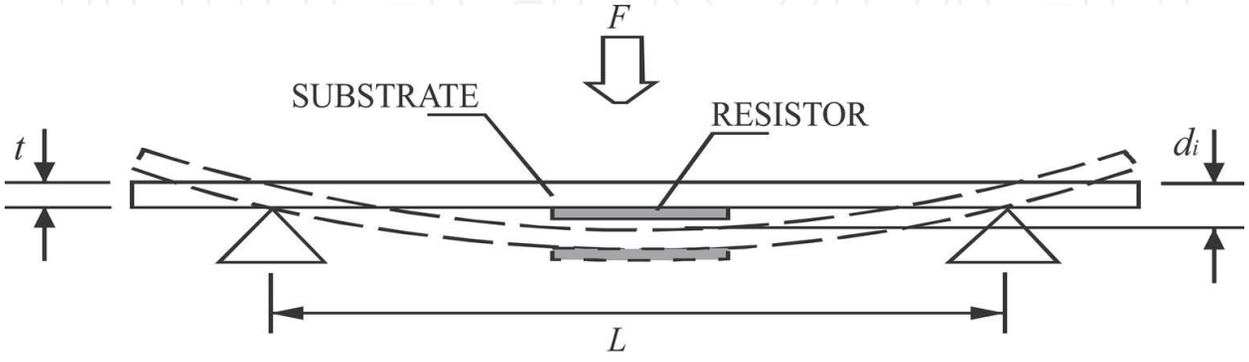

Figure 1. Schematic presentation of mechanically strained thick-film resistor.

R_{sq} (kΩ/sq)	l (mm)	$\overline{R_i}$ (kΩ)	$\overline{\lvert \Delta R/Ri \rvert}$ (%)	$\overline{GF}$	$\overline{NI}$ (dB)	$\overline{\Delta l}$ (μm)
1	2	0.666	0.401	4.2	−19.5	1.905
1	4	1.290	0.333	3.5	−26.6	3.81
1	6	1.49	0.303	3.2	−29.6	5.715
10	2	16.595	0.958	10.06	−20	1.905
10	4	32.81	0.945	9.92	−19.5	3.81
10	6	50.644	0.918	9.64	−19.1	5.715
100	2	276.51	1.381	14.50	−1.8	1.905
100	4	495.83	1.266	13.30	−7.3	3.81
100	6	704.3	1.136	11.92	−10.3	5.715

Table 1. Experimental data (nominal sheet resistance R_{sq}, resistor length l, mean value of initial resistance R_i, relative resistance change due to mechanical straining $\Delta R/R_i$, gauge factor GF, noise index NI and resistor length change Δl) for thick-film resistors with different geometries (width: w = 1 mm, length: l = 2, 4 and 6 mm) subjected to maximal mechanical straining of 400 μm [16].

breakthrough or influence the height of glass barriers that exist between adjacent conducting particles. It can only affect widths of glass barriers present in the film, thus changing the barrier resistance. Alteration of charge transport parameters also reflects on measured noise index values. Noise index values are decreasing with increasing resistor length and increasing for resistors realized with compositions with higher sheet resistances. Thick-film resistors realized using 10 kΩ/sq compositions usually have GF ~10 and stable NI values and therefore are commonly used as strain sensors.

3. Electrically strained thick-film resistive structures

Different conditions of thick-film resistor application that induced the need to investigate their behaviour under stress also brought to attention the importance of high-voltage pulse stressing. The most of the available data dealt with trimming of thick resistive films by the energy of high-voltage pulses [6–8], a trimming method based on internal discharges using both thick-film resistor terminations as electrodes for applying the high-voltage energy to the resistor body. Also, several papers explored properties of low-ohm thick-film surge resistors [9] that serve as protection of communication systems. However, little attention has been paid to the influence of high-voltage pulse stressing on structure and noise performances of conventional thick-film resistors [20, 21].

High voltage pulse stressing of thick resistive film causes irreversible resistance change. Experimental data obtained by extensive investigations of performances of thick-film resistors subjected to this type of straining [20, 21] showed that behaviour under strain strongly depends

on sheet resistances of resistor compositions used. Resistors based on compositions with low sheet resistances exhibit macro-structural changes that result in irreversible resistance increase. Lack of micro-structural changes is a consequence of the dominant conducting mechanism, conducting through clusters of conducting particles. High-voltage treatment leads to burning and evaporation of the resistive layer. Resistor volume is reduced causing the significant resistance and noise index increase (**Figure 2**).

Resistors realized using compositions with medium values of sheet resistances exhibit initial resistance decrease followed by the significant resistance increase during high voltage pulse stressing (**Figure 3**). Lower pulse amplitudes lead to resistance decrease due to changes in conducting mechanisms, metallic conduction through conducting particles and sintered contacts and tunnelling through glass barriers. High-voltage treatment affects charges captured by traps present in thin glass layers between neighbouring conducting particles or the trap concentration increases [12] due to existence of impurities introduced in insulating layers during firing. In addition, a minor resistance decrease may occur due to the conversion of single chain from non-conductive to conductive state. High-voltage treatment induces electrical field inside MIM unit that is insufficient to provoke dielectric breakthrough and therefore decrease of the resistance due to the increase in a number of contacts between neighbouring particles does not occur. Measured resistances substantially increase when the pulse voltage reaches the critical point when macro-structural changes occur. High-voltage treatment leads to burning and evaporation of the resistive layer thus reducing its volume and causing significant resistance increase similar to the one seen in resistors based on compositions with low sheet resistances. Since the low-frequency noise in thick-film resistors is the consequence of electrical charge transport fluctuations, noise index values are in agreement with resistance behaviour (**Figure 3**). Due to high voltage treatment, conduction is being modulated by electrical charges captured by traps that are not directly involved in conduction, thus altering the height of the potential barriers of MIM units. For these reasons, measured noise index values are more sensitive to changes on micro-structural level than resistance.

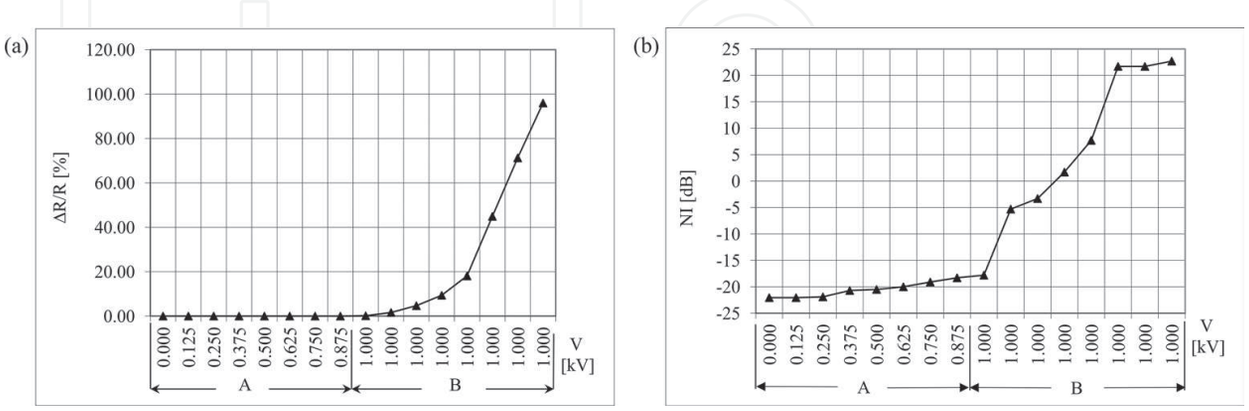

Figure 2. Experimental results. (A) Multiple series of 10 pulses with increasing amplitudes, (B) single pulses of the critical amplitude for relative resistance (a) and noise index (b) changes during high-voltage pulse stressing of 1 kΩ/sq thick-film resistor (resistor width: w = 1 mm, length: l = 3 mm) [21].

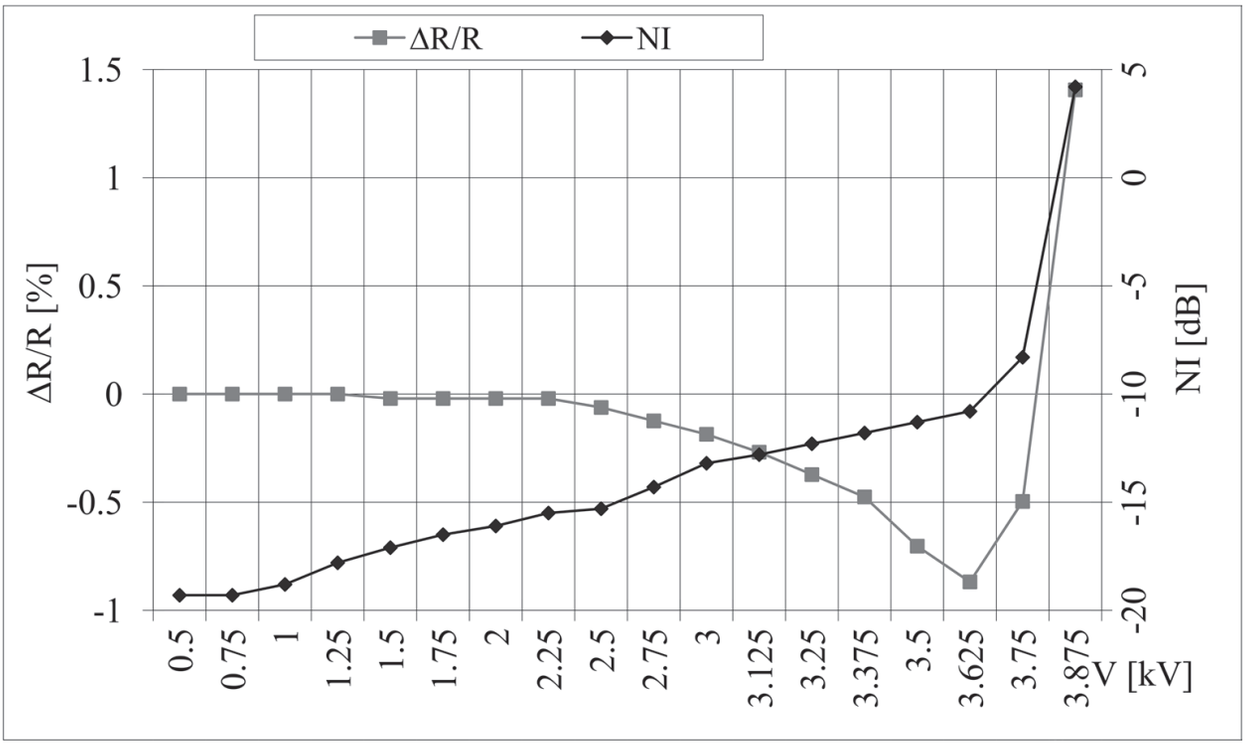

Figure 3. Experimental results for relative resistance and noise index changes during high voltage pulse stressing of 10 kΩ/sq thick-film resistor using multiple series of 10 pulses with increasing amplitudes (resistor width: w = 1 mm, length: l = 3 mm) [21].

Established correlation between structural properties and low-frequency noise can also be illustrated using noise spectra measurements (**Figure 4**). The fitting of experimental results for current noise spectra and the following theoretical relation can be performed:

$$S_I(f) = A_0 + \frac{B_0}{f^{\gamma}} + \sum_i \frac{C_i}{2\pi f_{Ci}(1 + f^2/f_{Ci}^2)}. \tag{4}$$

The first term is the thermal current noise given by:

$$A_0 = \frac{4 k_B T}{R}, \tag{5}$$

where k_B is the Boltzmann's constant, T is the absolute temperature and R is the resistance of thick resistive film. 1/f noise is represented by the second term where B_0 and γ are fitting parameters. The sum of noise spectra of the Lorentzian shape is presented by the third term where C_i and f_{Ci} are characteristic parameters and frequencies, respectively.

1/f noise is the dominant noise component in the total current noise spectrum. Fitting parameters B_0 and γ can be used in determining its sensitivity to high-voltage treatment. Fitting parameter γ has value γ = 1 both before and after the performed straining. **Figure 5** shows current dependencies of B_0. Parameter B_0 increases for approximately one order of magnitude with applied

http://dx.doi.org/10.5772/intechopen.69441

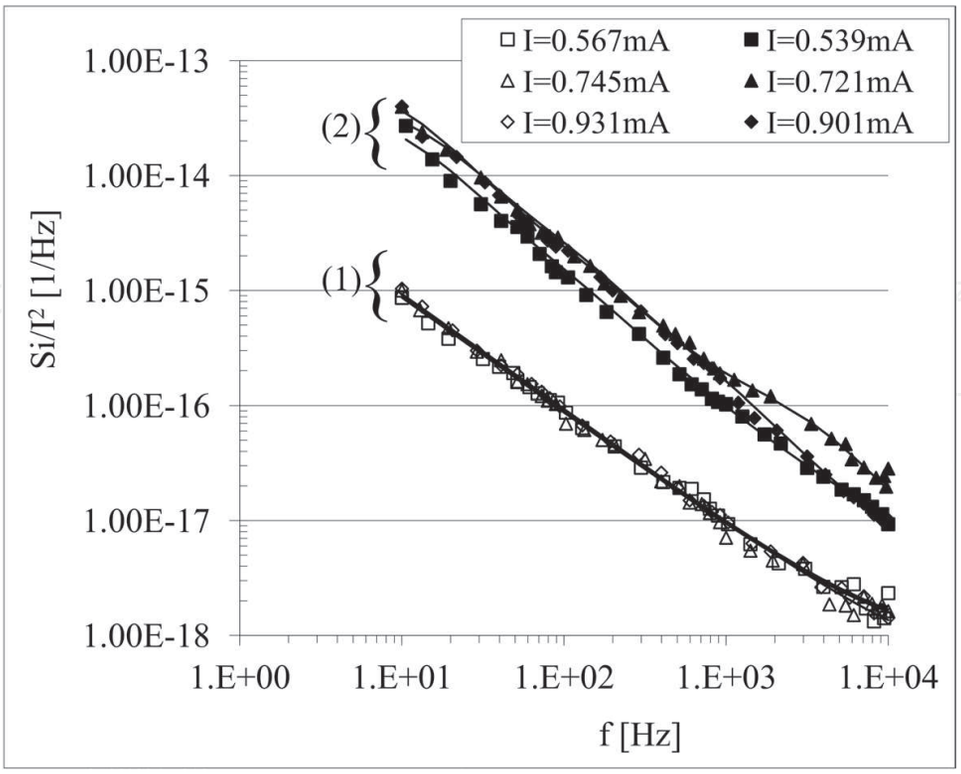

Figure 4. Experimental results for normalized current noise spectra before (1) and after (2) high voltage pulse stressing (multiple series of 10 pulses with increasing amplitudes) for 10 kΩ/sq thick-film resistor (full lines, fitting results) [21].

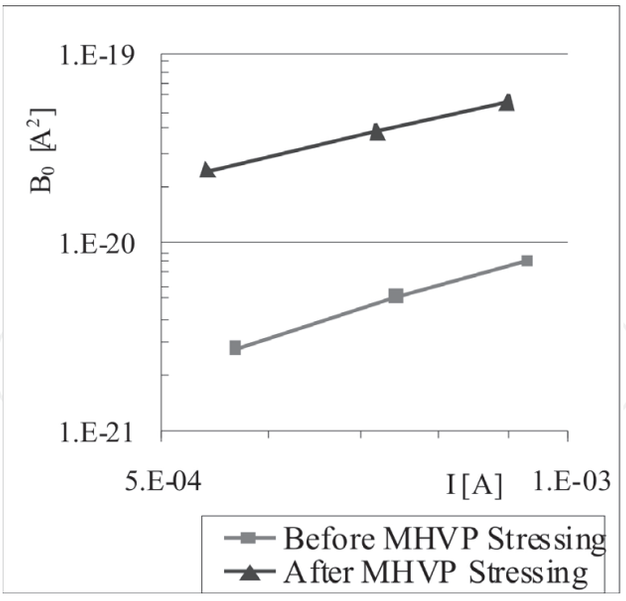

Figure 5. 1/*f* noise fitting parameter B_0 before and after high voltage pulse stressing of 10 kΩ/sq thick-film resistors [21].

stressing and the current dependence $B_0 \sim I^a$, with exponent $a > 2$ before and $a < 2$ after stressing. Contribution of noise due to mobility fluctuations in clusters and contacts between particles to total 1/*f* noise after high voltage pulse straining are possible causes of the exponent '*a*' change.

Normalized noise amplitude B_0/I^2 before and after high-voltage pulse stressing is shown in **Figure 6**. The normalized noise amplitude is dimensionless in opposition to fitting parameter B_0. Analogous to data given in **Figure 5**, 1/*f* noise increases for about an order of magnitude with applied high-voltage treatment. After performed fitting procedure, Lorentzian terms caused by fluctuations induced by the presence of traps in insulating layers of MIM units can be observed as slight bends of current noise spectra. Although concealed by 1/*f* noise, Lorentzian terms affect the agreement of measured values and theoretical relation. Current noise spectra analyses, prior to and after high voltage pulse stressing, are in agreement with resistance and noise index behaviour. It is interesting to note that conducting mechanisms seen in resistors with medium sheet resistances combine conducting mechanisms observed in resistors with greater and lower contents of conducting phase. Low-frequency noise measurements that include current noise spectrum and noise index measurements provide results that are far more sensible to macro- and micro-structural changes than measured resistance values. This fact is of special importance in reliability analysis when reversible changes of resistance occur due to straining of thick resistive films.

When thick-film resistors based on high sheet resistance compositions are concerned, due to a low volume fraction of the conducting phase, dominant conduction mechanism is tunnelling through glass barriers. Stressing causes pronounced micro-structural changes, changes barrier resistances and causes significant resistance decrease similar to the ones seen in resistors based medium sheet resistance compositions. Experimental data showed that noise index values are in agreement with resistance behaviour exhibiting an increase of *NI* values with the resistance progressive decrease and reaching their constant values (saturation) with a stagnation of the resistance decrease (**Figure 7**).

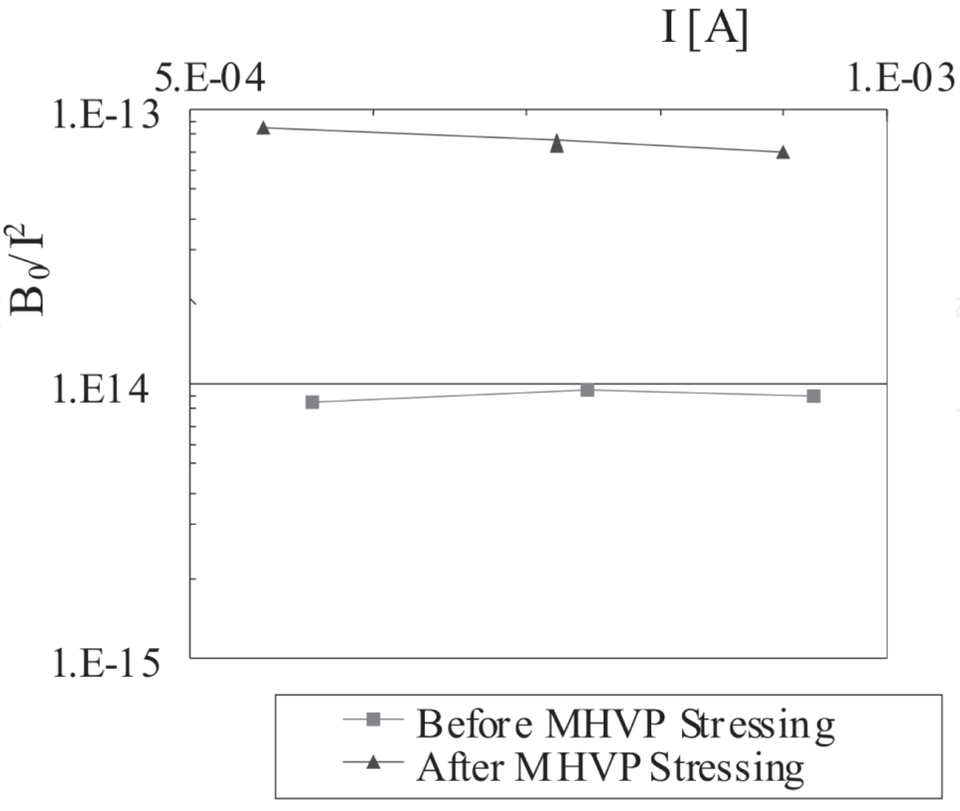

Figure 6. Normalized noise amplitude before and after high voltage pulse stressing of 10 kΩ/sq thick-film resistors [21].

http://dx.doi.org/10.5772/intechopen.69441

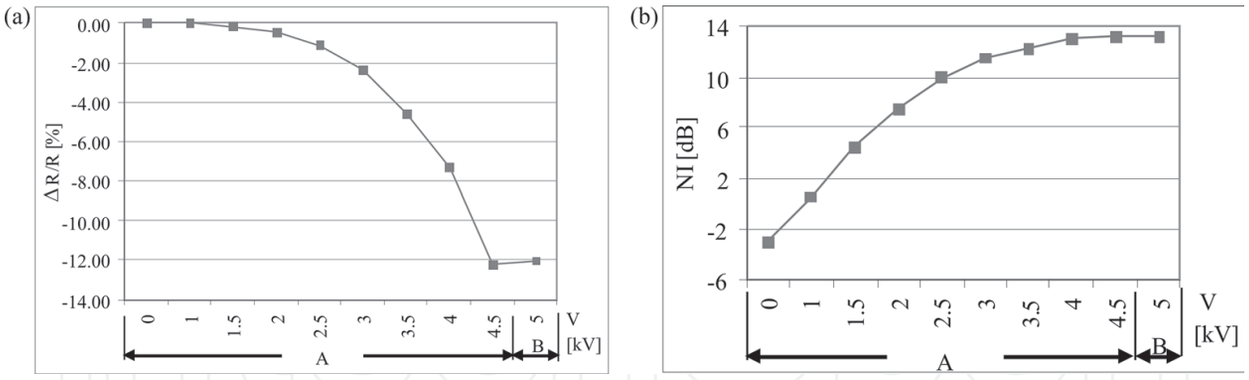

Figure 7. Experimental results. (A) Multiple series of 10 pulses with increasing amplitudes, (B) single pulses of the critical amplitude for relative resistance (a) and noise index (b) changes during high-voltage pulse stressing of 100 kΩ/sq thick-film resistors (resistor width: w = 1 mm, length: l = 3 mm) [21].

4. Simultaneous mechanical and electrical straining

Investigations of mechanical and electrical straining of thick-film resistors showed that these two types of straining have opposite effects on behaviour of these complex nanostructures [5, 20, 21]. Examining effects of the simultaneous impact of mechanical and electrical straining on thick-film resistors [16] is of particular interest for sensitive equipment exploitation since simultaneous mechanical and electrical straining may affect resistors capability to withstand high-voltage treatment.

In the case of medium and high sheet resistance compositions, resistance changes of thick resistive films exposed to high-voltage treatment are caused by changes in the micro-structural level [20] that result in decreasing resistance values. In a case of thick-film resistors subjected to mechanical straining, resistance changes are caused by changes in physical dimensions and more dominantly by changes on micro-structural level resulting in increasing resistance values [5, 16]. On the other hand, simultaneous mechanical and electrical straining has opposing effects on performances of thick-film resistors [16]. The ratio of conducting and insulating phase determines sheet resistances of thick resistive films and accordingly micro-structural properties and charge transport conditions. When compositions with a high content of conducting phase are in question, metallic conduction is the dominant conducting mechanism. When the simultaneous impact of these two types of straining are in question, they have opposing effects on tunnelling through insulating layers of MIM unit and accordingly on barrier resistances. In a case of applied mechanical straining, widths of glass barriers are being altered. On the other hand, applied electrical straining affects glass barrier heights. Taking into account the fact that tunnelling is not a dominant conducting mechanism when thick-film resistors with low sheet resistances are concerned, the lack of micro-structure changes is expected. Simultaneous mechanical and electrical straining cause changes in the macro-structure. High-voltage pulse stressing causes visible vaporisation of resistive layers. It decreases volumes of resistors and therefore significantly increases their resistances. Gauge factor changes exhibit increase following the shapes of curves of the resistance changes due to resistor degradation. Noise index values are in agreement with resistance behaviour and show significant increase confirming the fact that noise parameters are very sensitive to structural changes of thick-film resistors, more sensitive than resistance changes (**Figure 8**).

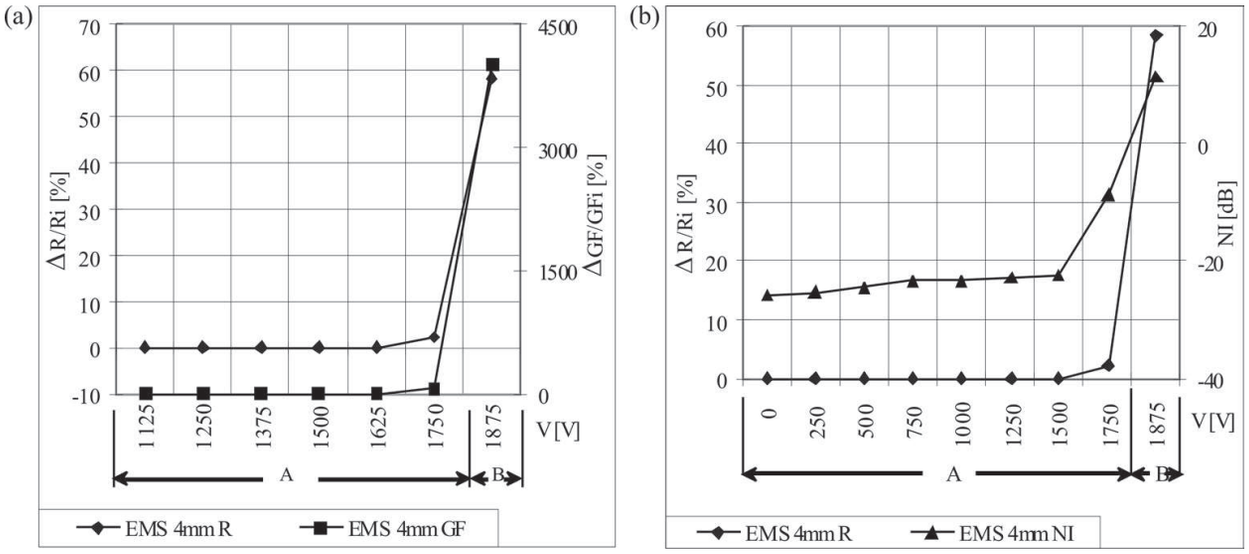

Figure 8. Experimental results for relative resistance, gauge factor changes (a) and noise index (b) for simultaneously mechanically and electrically strained 1 kΩ/sq thick-film resistors (resistor width: $w = 1$ mm, length: $l = 4$ mm) [16].

In a case of resistor compositions with medium sheet resistances, conduction incorporates both tunnelling through glass barriers and metallic conduction. Change of barrier resistance results in decreasing resistance values that is being succeeded by increasing resistance values caused by alterations on macro-structural level analogous to ones observed in low sheet resistance compositions. *GF* values are stable until degradations on macro-structure level occur and onwards follow the shapes of curves of the resistance changes. Noise index values are very sensitive, registering both micro- and macro-structural degradations of strained thick-film resistors. Experimental results for relative resistance, gauge factor changes and noise index for simultaneously mechanically and electrically strained 10 kΩ/sq thick-film resistors are given in **Figure 9(a)** and **(b)** [16]. In order to illustrate effects of electrical straining alone and simultaneous mechanical and electrical straining, the summary plot for relative resistance change of 10 kΩ/sq resistors is given in **Figure 9(c)** [16]. Figure shows that decreasing resistance values due to changes on micro-structural level are observed in the case of electrically strained and simultaneously electrically and mechanically strained thick-film resistors. Glass barrier height irreversibly changed [20], thus changing barrier resistance value due to applied high-voltage treatment. During simultaneous impact of two different types of straining, glass barriers were affected in two opposing manners: mechanical straining reversibly altered barrier width while electrical straining irreversibly affected barrier height. These opposing effects seem to enhance the ability of thick resistive film to endure high-voltage treatment by extending its lifetime to failure.

In the case of high sheet resistance resistor compositions, small conducting/isolating phase ratio determines dominant conducting mechanism-tunnelling through glass barriers. This small volume fraction of conducting phase leads to pronounced micro-structure changes, changing barrier resistances and causing significant resistance decrease. Gauge factor changes show an increase with the applied straining as well as noise index values. Experimental results for relative resistance, gauge factor changes and noise index for simultaneously mechanically and electrically strained 100 kΩ/sq thick-film resistors are given in **Figure 10**.

http://dx.doi.org/10.5772/intechopen.69441

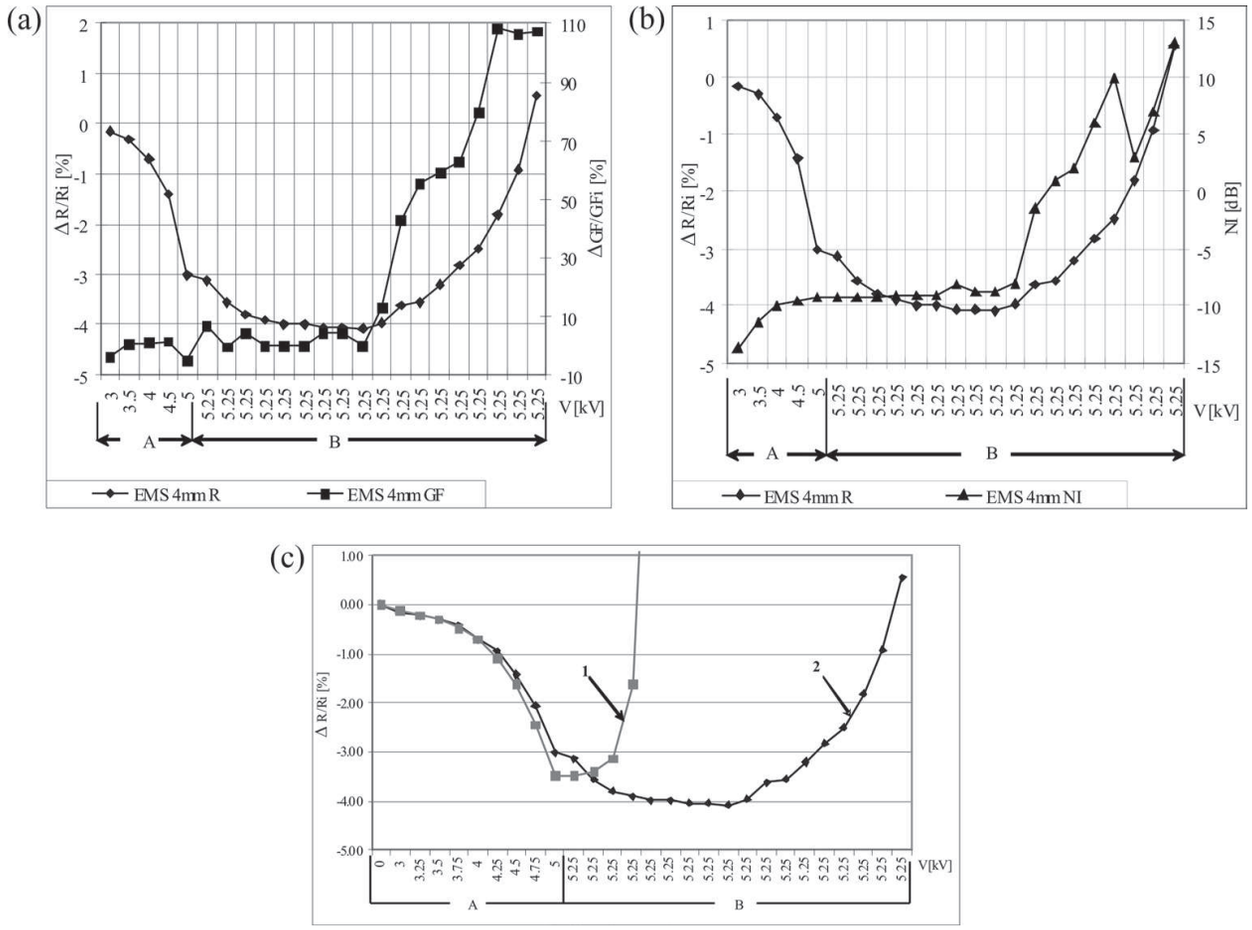

Figure 9. Experimentally obtained results for relative resistance, gauge factor changes (a) and noise index (b) for thick resistive films subjected to simultaneous impact of mechanical and electrical straining along with summary plot of relative resistance change (c) for electrically (1) and simultaneously mechanically and electrically strained (2) 10 kΩ/sq thick-film resistors (A—10 pulses per series, B—single pulses, resistor width: w = 1 mm, length: l = 4 mm) [16].

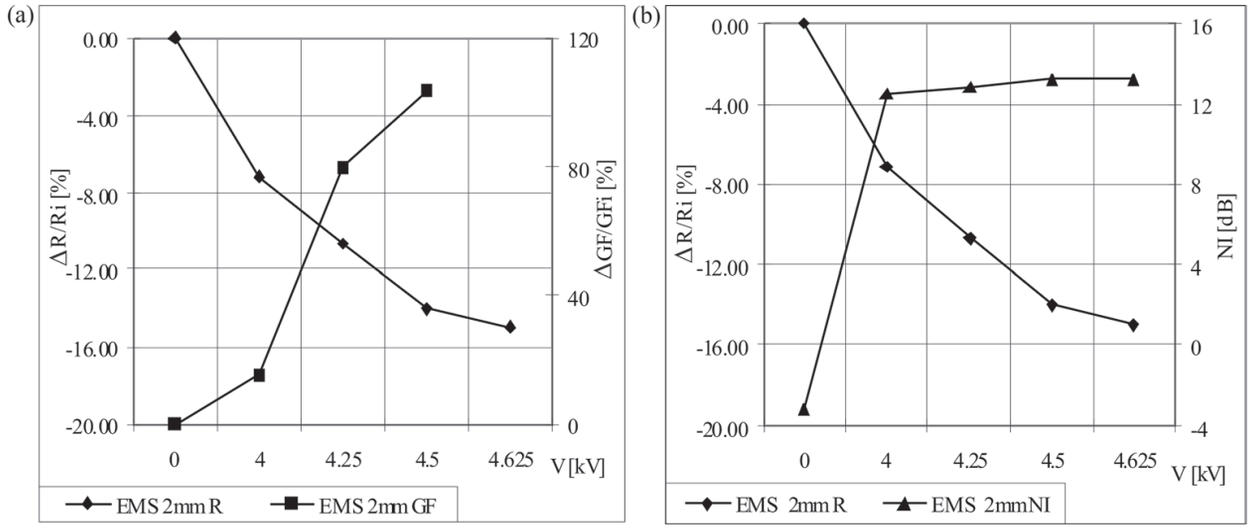

Figure 10. Experimental results for relative resistance, gauge factor changes (a) and noise index (b) for simultaneously mechanically and electrically strained (10 pulses per series) 100 kΩ/sq thick-film resistors (resistor width: w = 1 mm, length: l = 2 mm) [16].

Sources of low-frequency noise in thick resistive films are correlated to charge transport mechanisms [11]; metallic conduction is correlated to resistance fluctuations of contact resistivity and particle resistivity and tunnelling through glass barriers is correlated to noise due to modulation of the Nyquist noise and fluctuations induced by existence of traps in insulating layers of MIM units. **Figure 11** shows experimental results for current noise spectrum before and after simultaneous electrical and mechanical straining of thick resistive films whose experimental results for relative resistance, gauge factor and noise index changes are given in **Figure 9** [16]. Presented data demonstrate that changes on micro-structural level cause initial resistance decrease. Changes on macro-structural level have an opposing effect. Initial resistance decrease is being followed by resistance increase, thus reaching the initial resistance value.

In order to fully comprehend effects correlated to a current noise of simultaneously strained thick resistive films, the fitting procedure was implemented based on experimental data presented in **Figure 11** and theoretical relation (4). As an illustration, the fitting and experimental results for the curve (4) in **Figure 11**, together with contributions of different kinds of noise sources in the total current noise spectrum, are given in **Figure 12**.

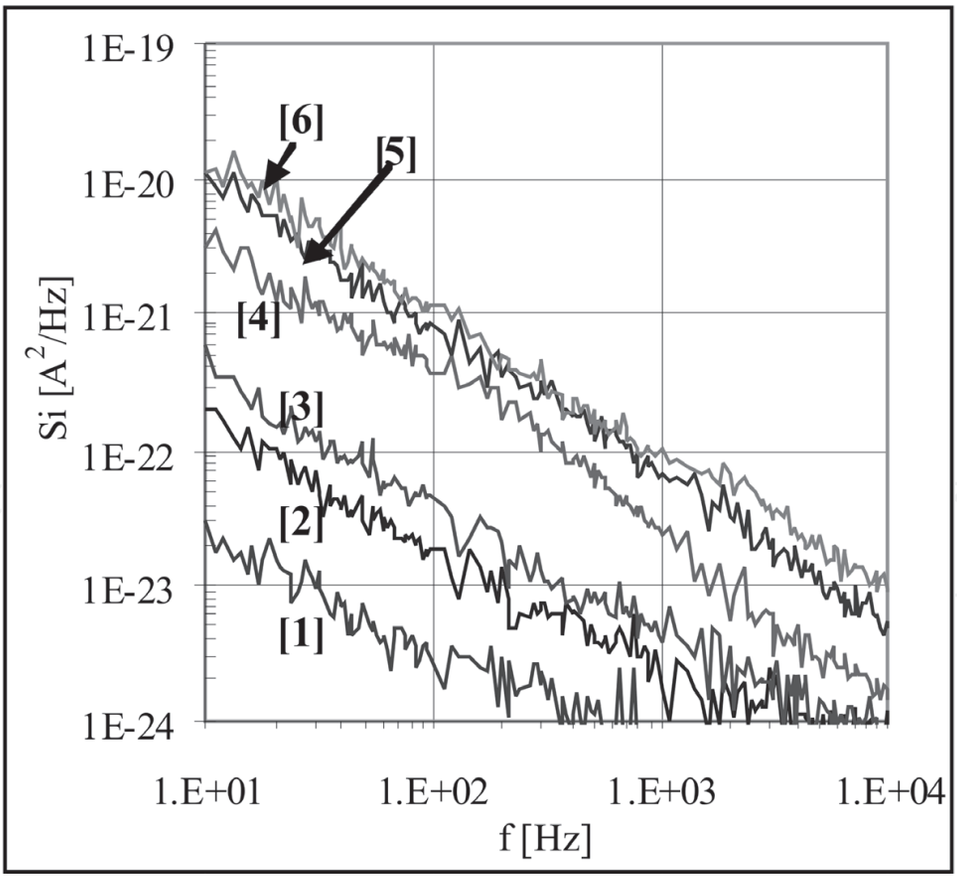

Figure 11. Experimental results for current noise spectrum before (1—I = 0.1488 mA, 2—I = 0.2925 mA, 3—I = 0.4452 mA) and after (4—I = 0.1435 mA, 5—I = 0.2917 mA, 6—I = 0.4424 mA) simultaneous mechanical and electrical straining of 10 kΩ/sq thick-film resistors [16].

http://dx.doi.org/10.5772/intechopen.69441

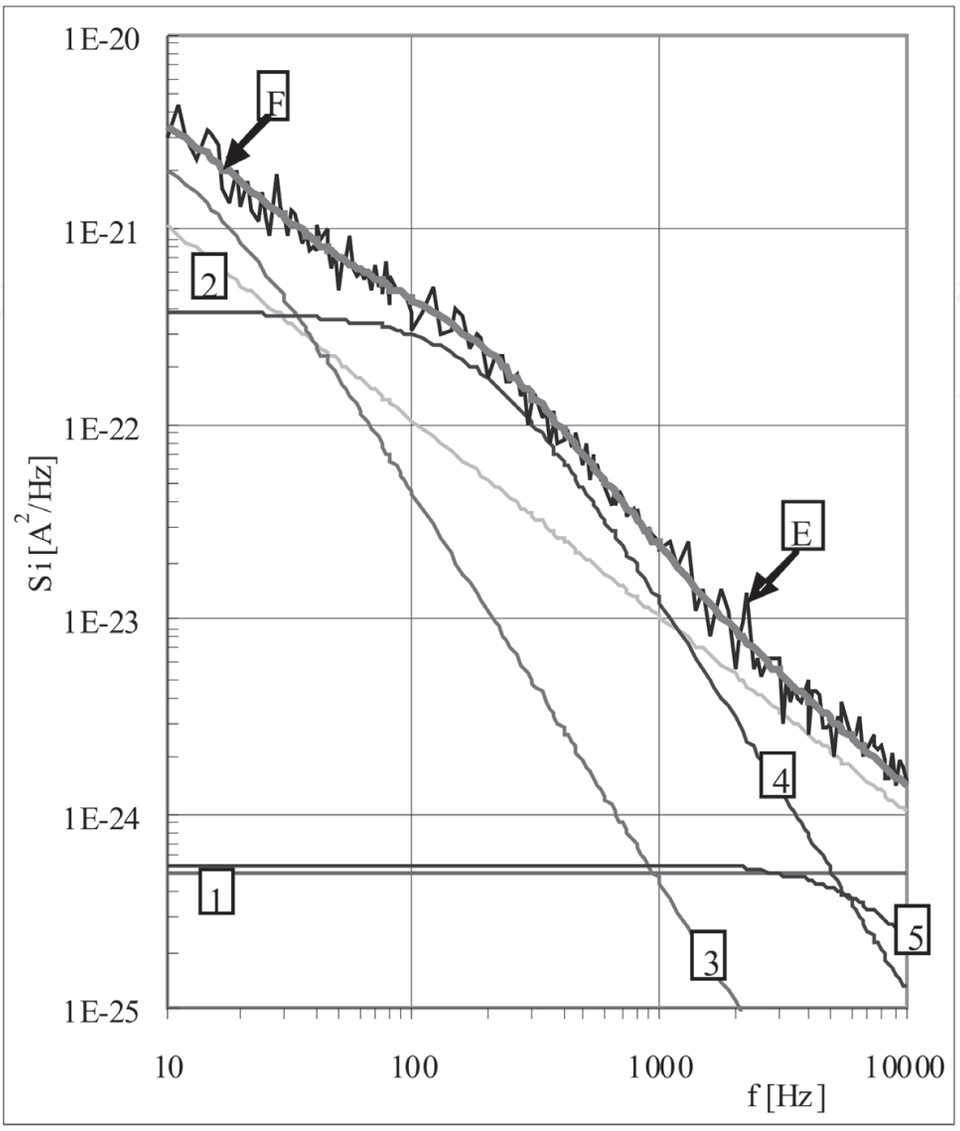

Figure 12. Experimental results (*E*) for current noise spectrum and fitting results (*F*) according to Eq. (4) for curve (4) in **Figure 8** with contributions of different kinds of noise sources in the total current noise spectrum (1—thermal current noise, 2—1/*f* noise, 3, 4, 5—noise spectra of the Lorentzian shape) [16].

In the total current noise spectrum, dominant 1/*f* noise includes 1/*f* noise due to particle and contact resistivity fluctuations and fluctuations of potential barrier height caused by Nyquist noise of the insulator [13, 22]. Effects of simultaneous electrical and mechanical straining on 1/*f* noise can be evaluated using 1/*f* noise fitting parameters γ and B_0. It is found that fitting parameter γ has value 1 both before and after simultaneous mechanical and electrical straining while B_0 values are presented in **Figure 13**.

It can be seen that parameter B_0 increases for approximately one order of magnitude with applied straining. The current dependence $B_0 \sim I^a$, with exponent $a > 2$ before and $a < 2$ after stress is found. This change of the exponent '*a*' could be explained by a greater participation of noise caused by mobility fluctuations in clusters and particles contacts in total 1/*f* noise after stressing. Presence of traps in insulating layers of MIM units is related to Lorentzian

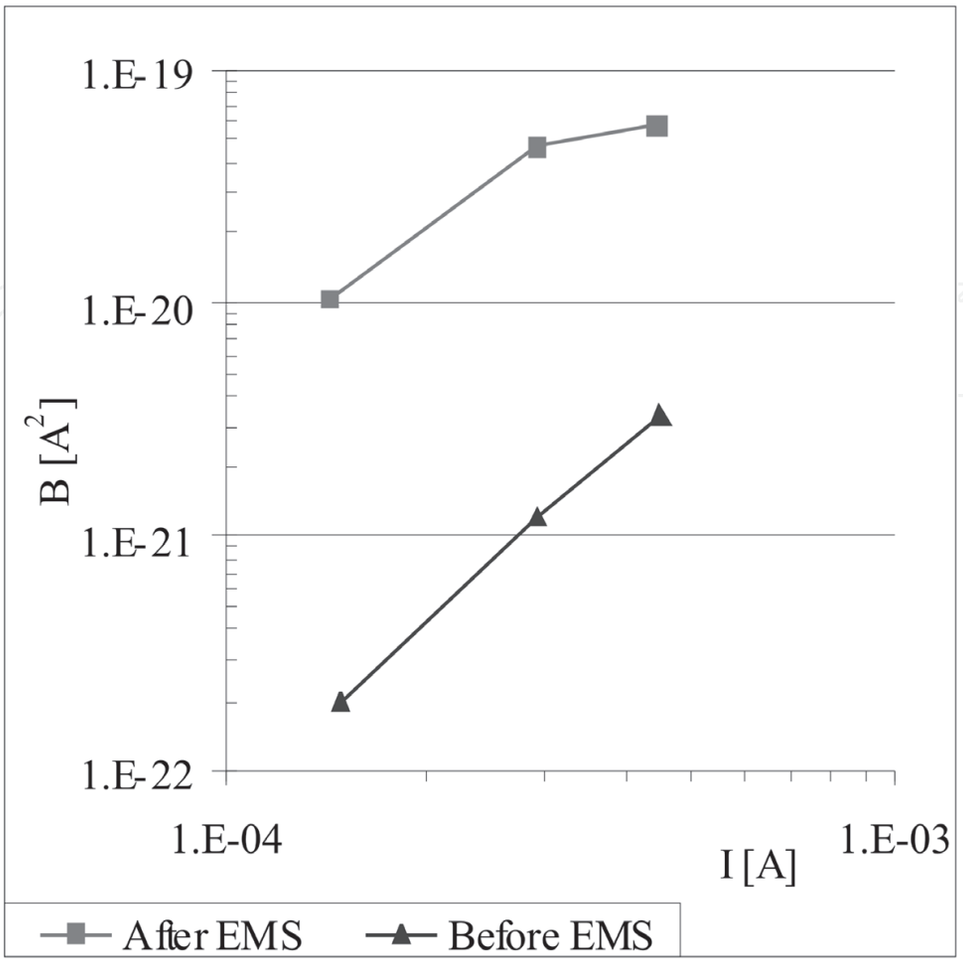

Figure 13. 1/*f* noise parameter B_0 before and after simultaneous mechanical and electrical straining of 10 kΩ/sq thick-film resistors (resistor width: w = 1 mm, length: l = 4 mm) [16].

terms present in the total noise spectrum of thick resistive films. Presence of these terms is confirmed by data presented in [23]. Based on current noise spectra measurements of simultaneously electrically and mechanically strained resistors, detailed experimental and numerical analysis proved that straining affects the shape and the level of the noise spectra. Therefore, low-frequency noise parameters are sensitive to degradations induced by applied straining. Obtained results, being in accordance with measured noise index values, are significant for contemporary sensitive applications of thick resistive films. In cases of reversible resistance changes that often disguise degradation processes in thick-film resistors, low-frequency noise measurements can be used as useful tools in detecting the ongoing reliability issues.

5. Conclusion

In the fabrication of precise and reliable up-to-date communication systems stability and precise resistance values of widely utilized conventional thick-film resistors are of great importance. Different conditions of their application induced the need to investigate their behaviour under

stress, especially under influence of mechanical and electrical straining. Mechanical straining leads to reversible resistance change due to change of charge transport conditions. It predominantly affects tunnelling through glass barriers by changing barrier widths. Electrical straining leads to irreversible resistance change due to barrier height alteration. Simultaneously, mechanically and electrically strained resistors are affected in two opposing manners; mechanical straining reversibly alters barrier widths while electrical straining irreversibly affects barrier heights. Having in mind that tunnelling through glass barriers is primarily affected by simultaneous straining; an impact of the simultaneous straining can be optimally evaluated using resistors with medium sheet resistances that include both metallic conduction and tunnelling through glass barriers. Results presented in this chapter can be viewed as an experimental verification of correlation between resistance, gauge factor and low-frequency noise parameters (noise index and current noise spectra) and changes with resistor degradation due to the impact of these three types of straining. Furthermore, they can be seen as validation of earlier presumptions [24, 25] that standard resistance, noise spectrum and noise index measurements are valuable tools in reliability evaluation of thick resistive films.

Acknowledgements

The authors would like to thank the Ministry of Education, Science and Technological Development of the Republic of Serbia for supporting this research within projects III44003 and III45007.

Author details

Zdravko Stanimirović

Address all correspondence to: zdravkos@iritel.com

Institute for Telecommunications and Electronics, IRITEL a.d. Beograd, Belgrade, Republic of Serbia

References

[1] Prudenziati M, Morten B, Taroni A. Characterization of thick-film resistor strain gauges on enamel steel. Sensors and Actuators. 1982;**2**:17-27. DOI: 10.1016/0250-6874(81)80025-X

[2] Hrovat M, Belavič D, Samardžija Z, Holc J. A characterization of thick film resistors for strain gauge applications. Journal of Materials Science. 2001;**36**(11):2679-2689. DOI: 10.1023/A:1017908728642

[3] Canalli C, Malavasi D, Morten B, Prudenziati M, Taroni A. Piezoresistive effects in thick-film resistors. Journal of Applied Physics. 1980;**51**(6):3282-3288. DOI: 10.1063/1.328035

[4] Shah JS. Strain sensitivity of thick-film resistors. IEEE Transactions on Components, Packaging, and Manufacturing Technology. 1980;**3**(4):554-564. DOI: 10.1109/TCHMT.1980.1135645

[5] Stanimirović Z, Jevtić MM, Stanimirović I. Performances of conventional thick-film resistors subjected to mechanical straining. In: Proceeding of the 24th International Conference on Microelectronics, Niš, Serbia. 2004;**2**:675-678. DOI: 10.1109/ICMEL.2004.1314920

[6] Dziedzic A, Kolek A, Ehrhardt W, Thust H. Advanced electrical and stability characterization of untrimmed and variously trimmed thick-film and LTCC resistors. Microelectronics Reliability. 2006;**46**:352-359. DOI: 10.1016/j.microrel.2004.12.014

[7] Stanimirović Z, Stanimirović I. Effects of high voltage pulse trimming on structural properties of thick-film resistors. Science of Sintering. 2017;**49**:91-98. DOI: 10.2298/SOS1701091S

[8] Stanimirović I, Stanimirović Z. Influence of HVP trimming on primary parameters of thick resistive films. Journal of Materials Science: Materials in Electronics. 2017;**28**:8002-2010. DOI: 10.1007/s10854-017-6504-7

[9] Barker MF. Low ohm resistor series for optimum performance in high voltage surge applications. Microelectronics International. 1997;**43**:22-26. DOI: 10.1108/13565369710800493

[10] Kolek A, Ptak P, Dziedzic A. Noise characteristics of resistors buried in low-temperature co-fired ceramics. Journal of Physics D: Applied Physics. 2003;**36**:1009-1017. DOI: 10.1088/0022-3727/03/081009

[11] Mrak I, Jevtić MM, Stanimirović Z. Low-frequency noise in thick-film structures caused by traps in glass barriers. Microelectronics Reliability. 1998;**38**:1569-1576. DOI: 10.1016/S0026-2714(98)00032-8

[12] Jevtić MM, Stanimirović Z, Mrak I. Low-frequency noise in thick-film resistors due to two-step tunneling process in insulator layer of elemental MIM cell. IEEE Transactions on Components and Packaging Technologies. 1999;**22**(1):120-125. DOI: 10.1109/6144.759361

[13] Kusy A, Szpytma A. On 1/*f* noise in RuO_2-based thick resistive films. Solid-State Electron. 1986;**29**:657-665. DOI: 10.1016/0038-1101(86)90148-6

[14] Arshak KI, McDonagh D, Durcan MA. Development of new capacitive strain sensors based on thick film polymer and cermet technologies. Sensors and Actuators A: Physical. 2000;**79**(2):102-114. DOI: 10.1016/S0924-4247(99)00275-7

[15] Tankiewicz S, Morten B, Prudenziati M, Golonka LJ. New thick-film material for piezoresistive sensors. Sensors and Actuators A: Physical. 2001;**95**(1):39-45. DOI: 10.1016/S0924-4247(01)00754-3

[16] Stanimirović Z, Jevtić MM, Stanimirović I. Simultaneous mechanical and electrical straining of conventional thick-film resistors. Microelectronics Reliability. 2008;**48**:59-67. DOI: 10.1016/j.microrel.2006.09.039

[17] Puers B, Sansen W, Paszczynski S: Assessment of thick-film fabrication method for force (pressure) sensors. Sensors and Actuators. 1987;**12**:57-76. DOI: 10.1016/0250-6874(87)87006-3

[18] Stanimirović Z, Jevtić MM, Stanimirović I. Computer simulation of thick-film resistors based on 3D planar RRN model. In: Proceedings EUROCON Belgrade, Serbia. 2005; **R24**:1687-1690. DOI: 10.1109/EURCON.2005.1630297

[19] Grimaldi C, Ryser P, Strassler S. Gauge factor enhancement driven by heterogeneity in thick-film resistors. Journal of Applied Physics. 2001;**91**(1): 322-327. DOI: 10.1063/1.1376672

[20] Stanimirović I, Jevtić MM, Stanimirović Z. High-voltage pulse stressing of thick-film resistors and noise. Microelectronics Reliability. 2003;**43**:905-911. DOI: 10.1016/S0026-2714(03)00094-5

[21] Stanimirović I, Jevtić MM, Stanimirović Z. Multiple high-voltage pulse stressing of conventional thick-film resistors. Microelectronics Reliability. 2007;**47**:2242-2248. DOI: 10.1016/j.microrel.2006.11.017

[22] Kleipenning TGM. On low-frequency noise in tunnel junctions. Solid-State Electron. 1982;**25**:78-79. DOI: 10.1016/0038-1101(82)90100-9

[23] Prudenziati M, Morten B, Masoero A: Excess noise and refiring processes in thick-film resistors. Journal of Physics D: Applied Physics. 1981;**14**:1355-1362. DOI: 10.1088/0022-3727/14/7/024

[24] Jevtić MM, Mrak I, Stanimirović Z. Thick-film resistor quality indicator based on noise index measurements. Microelectronics Journal. 1999;**30**:1255-1259. DOI: 10.1016/S0026-2692(99)00050-6

[25] Jevtić MM, Stanimirović Z, Stanimirović I. Evaluation of thick-film structural parameters based on noise index measurements. Microelectronics Reliability. 2001;**41**:59-66. DOI: 10.1016/S0026-2714(00)00207-9

IntechOpen